

Syntheses, Characterization and Optical Analysis of Ni(OH)₂ and NiO Nanopowders by using a Sonochemical Method

*Abedin Zebardasti, Fatemeh Rezaei, Sara Bagheri, and Alireza Aslani**

Department of Chemistry, Faculty of Sciences, Lorsetan University, Lorestan-Khoramabad, Iran.

Received: 2 Jun. 2014, Revised: 22 Nov. 2014, Accepted: 24 Jan. 2015.

Published online: 1 Jan. 2016.

Abstract: Ni(OH)₂ nanostructures were synthesized by the reaction of Ni(CH₃COO)₂·2H₂O and sodium hydroxide or tetramethylammonium hydroxide (TMAH) by a sonochemical method. Reaction conditions, such as the concentration of the Ni⁺² ions, aging time and power of the ultrasonic device played important roles in the size, morphology and growth process of the final products. The NiO nanoparticles were obtained by heating of Ni(OH)₂ nanoparticles at 500°C. The Ni(OH)₂ and NiO nanopowders were characterized by scanning electron microscopy (SEM), X-ray powder diffraction (XRD), solid state UV-vis, solid state photoluminescent and the Infrared spectroscopy (IR).

Keywords: Ni(OH)₂; NiO; Sonochemical; Nanoparticles.

1 Introduction

Nickel hydroxide “Ni(OH)₂” has been widely used as the active material of positive electrodes in many alkaline rechargeable batteries, such as Ni/Cd, Ni/H₂, Ni/MH, Ni/Fe, and Ni/Zn [1-4]. As inspired by both the potential application of Ni(OH)₂ and the novel properties of nanoscale materials, considerable efforts have recently been focused on the preparation of nanostructured Ni(OH)₂, such as nanotubes, nanorods, nanosheets and nanoribbons. Nevertheless, among the nanostructured Ni(OH)₂ previously reported, to the best of our knowledge, most were based upon zero- and one-dimensional nanoscale materials. They were always mixed into conventional spherical Ni(OH)₂ to be used [5-11] and could not independently used as the active materials in positive electrodes. Therefore, two- and three-dimensional Ni(OH)₂ hierarchical structures obtained by the self-assembly of low-dimensional building blocks have received increasing interest and can be independently used as the active materials in positive electrodes. As two-dimensional nanoscale materials, nanostructure-tured Ni(OH)₂ thin films are highly desired [12-17]. Nickel oxide (NiO) thin films are very prosperous materials with excellent electrochromic properties [18-20]. Other important applications of NiO films include preparation of alkaline batteries (as a cathode material), antiferromagnetic layers, p-type transparent conducting films [21, 22]. NiO thin films can be synthesized by thermal decomposition with Ni(OH)₂ thin film precursors. Liquid phase deposition (LPD) is one of the widely used techniques for synthesizing uniform metal hydroxide/oxide films, involving immersion of a substrate into an ammonia hydroxide solution containing metal-fluoro complex species and boric acid or an aluminum [23-27].

In the present work we have developed a simple sonochemical method to prepare NiO nanoparticles, wherein nickel hydroxide is synthesized as a precursor compound by the reaction of nickel acetate and sodium hydroxide (NaOH) in an ultrasonic device and is converted to NiO by heating at 500°C in a furnace. The Ni(OH)₂ and NiO nanostructures have been characterized by X-ray powder diffraction (XRD), IR spectroscopy and also the morphology and size of the nanostructures have been observed by scanning electron microscopy (SEM). We have performed these reactions in several conditions to find out the role of different factors such as the aging time of the reaction in the ultrasonic device and the concentration of the Ni⁺² ion on the morphology of the nanostructures.

2 Experimental

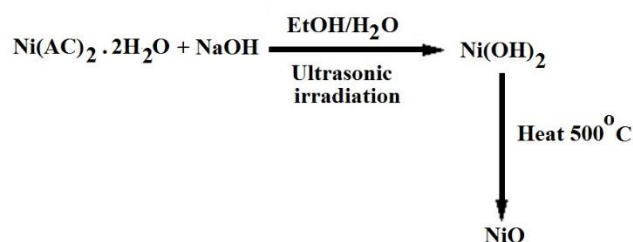
To prepare the Ni(OH)₂ precursor different amounts of NaOH solution with a concentration of 0.1 M were added to the 0.1,

*Corresponding author e-mail: a.aslani110@yahoo.com

0.2, 0.3 M solution of $\text{Ni}(\text{CH}_3\text{COO})_2 \cdot 2\text{H}_2\text{O}$ in ethanol. Then the suspension was ultrasonically irradiated with a high-density ultrasonic probe immersed directly into the solution under various conditions (Table 1). A multiwave ultrasonic generator (Sonicator-3000; Misonix, Inc., Farmingdale, NY, USA), equipped with a converter/transducer and titanium oscillator (horn), 10 mm in diameter, operating at 45 kHz with a maximum power output of 800 W, was used for the ultrasonic irradiation. The ultrasonic generator automatically adjusted the power level. The wave amplitude in each experiment was adjusted as needed. To form the MO powders the obtained precipitates were heated at 500°C in a furnace. X-ray powder diffraction (XRD) measurements were performed using a Philips diffractometer of X'pert Company with monochromatized $\text{Cu}_{\text{K}\alpha}$ radiation. The crystallite sizes of selected samples were estimated using the sherrer method. The samples were characterized with scanning electron microscope (SEM) (Philips XL 30) with gold coating. IR spectra were recorded on a SHIMADZU-IR460 spectrometer in KBr matrix. Optical absorption spectra of the powdered samples were recorded in a UV-VIS 1700 Shimadzu Spectrophotometer. The powdered sample were dispersed in ethyl alcohol and mounted in the sample chamber while pure ethyl alcohol was taken in the reference beam position. For photoluminescence measurement the samples were also taken in ethyl alcohol and the measurement were carried out in F-7000 Hitachi PL Spectrophotometer.

3 Results and Discussion

We can see the reaction between calcium acetate and NaOH to form calcium hydroxide and calcium oxide in scheme 1.



Scheme 1. The mechanism of NiO formation.

Table 1. Experimental condition for the preparation of $\text{Ni}(\text{OH})_2$.

sample	$\text{Ni}(\text{CH}_3\text{COO})_2 \cdot 2\text{H}_2\text{O}$	$\text{Ni}(\text{CH}_3\text{COO})_2 \cdot 2\text{H}_2\text{O}(\text{M})$	$\text{NaOH}(0.1\text{M})$	Agingtime	Ultrasound power
1	25(ml)	0.1	50 ml	1 hr	3-6 w
2	25(ml)	0.2	100 ml	1 hr	3-6 w
3	25(ml)	0.3	150 ml	1 hr	3-6 w
4	25(ml)	0.1	50 ml	30 min	3-6 w
5	25(ml)	0.1	50 ml	2 hr	3-6 w
6	25(ml)	0.1	50 ml	1 hr	12-15 w
7	25(ml)	0.1	50 ml	1 hr	36-39 w
8	50(ml)	0.1 + 2g PEG	100 ml	1 hr	3-6 w
9	25(ml)	0.1	25ml TMAH (0.2M)	1 hr	3-6 w
10	25(ml)	0.1+ 1g NaNO_3	50 ml	1 hr	3-6 w

Fig. 1a. shows the XRD pattern of a typical sample of $\text{Ni}(\text{OH})_2$ prepared by the sonochemical process in ethanol and Fig. 1b. shows the XRD pattern of the above samples after heating at 500°C . The obtained patterns match with the standard patterns of $\text{Ni}(\text{OH})_2$ and NiO.

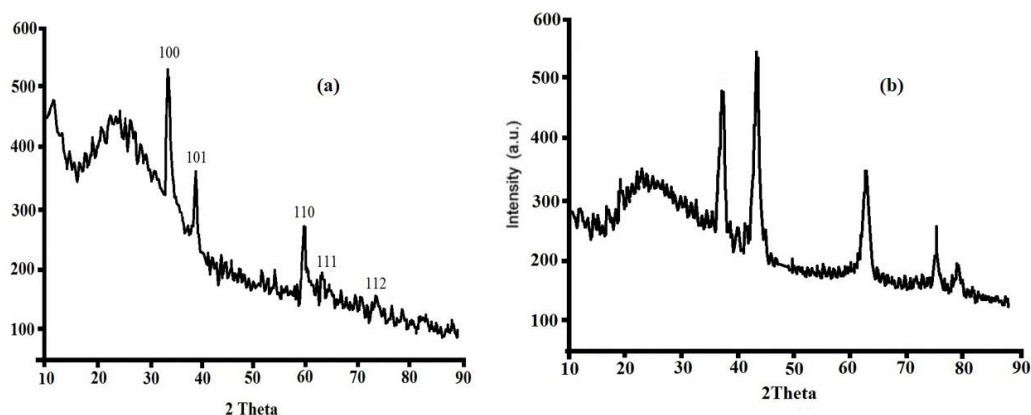


Figure 1. The XRD pattern of a) Ni(OH)₂ and b) NiO nanoparticles.

The crystalline phases of Ni(OH)₂ and NiO are respectively hexagonal and cubic, space groups P6₃cm and Fm3m with the lattice parameters $a = 3.5899 \text{ \AA}$, $c = 4.916 \text{ \AA}$, $z = 1$ for Ni(OH)₂ and $a = 4.81059 \text{ \AA}$ and $z = 4$ for NiO, which are close to the reported values. The sharp diffraction peaks of the sample indicated that well-crystallized Ni(OH)₂ and NiO crystals can be easily obtained under current synthetic condition. No characteristic peaks of other impurities have been detected, which indicated that the products are of high purity. The broadening of the peaks indicated that the particles were of nanometer scale. Estimated from the sherrer formula, $D = 0.891\lambda/\beta\cos\theta$, where D is the average grain size, λ is the X-ray wavelength (0.15405 nm), and θ and β are the diffraction angle and full-width at half maximum of an observed peak, respectively, the average size of the particles of sample number 1 “Ni(OH)₂ particles” was 32 nm and for above sample after heating at 500°C “NiO particles” was 70 nm which is in agreement with that observed from SEM images (Figure .3b).

The morphology, structure and size of the samples are investigated by Scanning Electron Microscopy (SEM). The effect of various parameters on the size and morphology of nanostructures was investigated in order to achieve the best structure. The concentration of the Ni²⁺ ion; Fig. 2a indicates the original morphology of the particles with the diameter varying between 30 to 90 nm. For investigation the role of concentration of Ni²⁺ ion in the morphology and size of the particles, the concentration was increased to 0.2 and 0.3 M (sample No. 2 and 3) according to fig. 2b and 2c, the particles obtained from above reactions have larger sizes than the obtained particles of sample No. 1.

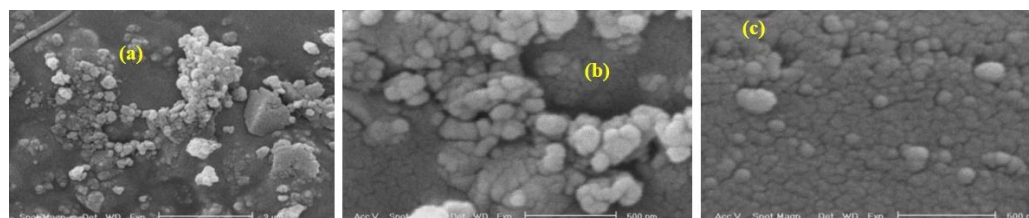


Figure 2. SEM images of Ni(OH)₂ nanoparticles for various Concentration of Ni²⁺ ion (a) sample No.1 (b) sample No.2 (c) sample No.3.

3.1. Aging Time

For understanding the effect of aging time on the morphology of the particles, the reaction carried out in 30 min, 1 h and 2 h. Fig. 3a shows the SEM images of the reaction that the aging time was 30 min (Sample No.4).

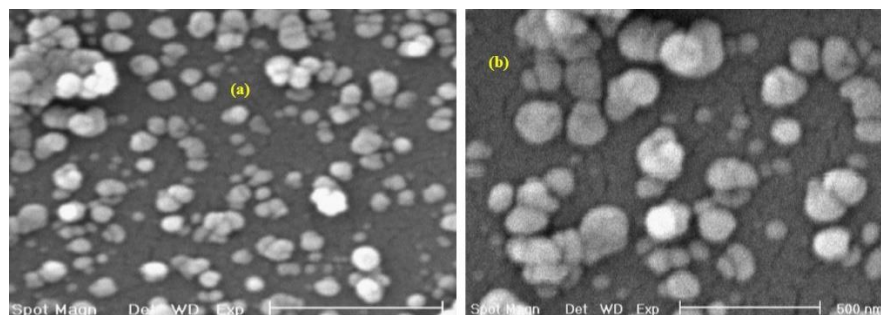


Figure 3. SEM images of Ni(OH)₂ nanoparticles for various aging time (a) sample No.4 (b) sample No.5.

Reference to Fig. 3a, when the aging time was decreased to 30 min, the obtained particles were bigger than the particles of

sample No. 1 that the aging time was 1 h, but when the aging time of reaction was increased to 2 hr we obtained nanoparticles with 60 nm in diameter, as described in Fig. 3b.

3.2 Power of Ultrasound Device

To investigate the role of sonicator device power, the reaction carried out in three various powers (samples No.1, 6 and 7). Fig. 4a shows the SEM images of the sample No. 6, as it can be seen, when the power was increased in the sample No. 6 we got the particles with nanometer size but the morphology was not changed. Fig. 4b shows the SEM images of the sample No.7. Comparing all of the above results, as it can be seen in fig. 4b, the best morphology with smaller particles and good distribution was obtained for the sample number 7 that the concentration of Ni^{+2} ion was 0.1 M, aging time was 1h and the ultrasound device power was increased to 45 W.

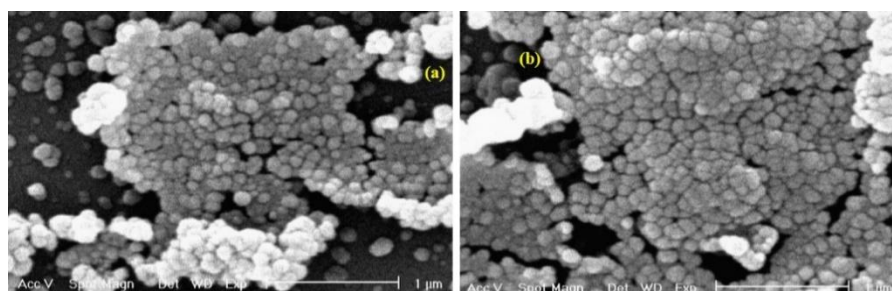


Figure 4. SEM images of $\text{Ni}(\text{OH})_2$ nanoparticles (a) sample No.6 (b) sample No.7

Fig. 5a shows the SEM image of the sample number 8 and the role of PEG on the morphology of this sample is obvious. It has been reported that the presence of a capping molecule (such as Poly Ethylene Glycol) can alter the surface energy of crystallographic surfaces, in order to promote the anisotropic growth of the nanocrystals. In this work PEG adsorbs on the crystal nuclei and it helps the $\text{Ni}(\text{OH})_2$ nanoparticles to grow separately.

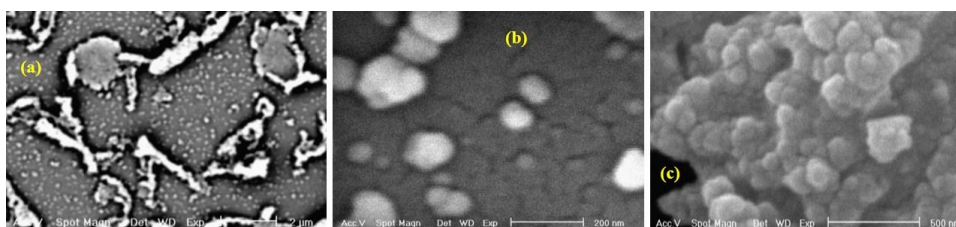


Figure 5. SEM images of $\text{Ni}(\text{OH})_2$ nanoparticles (a) sample No.8 (b) sample No.9 (c) sample No.10

We use TMAH as a weaker base for the reaction at optimized condition. As it can be seen in fig. 5b TMAH has no effect on the morphology of obtained nanostructures. For further investigation we use NaNO_3 at optimized condition. As it is shown in fig. 5c the nanoparticles grow separately and the nanostructures with suitable lengths and wide are obtained. The reaction was done without sonication for investigating the role of sonication on the morphology of product, as it has been seen in fig. 6a, the obtained particles did not have nano sizes. For further investigation, the reaction in optimized conditions was done in the presence of PEG without sonication for investigating the effect of stabilizer on the morphology of product. Comparing the result of this reaction (Fig. 6b) with Fig. 5a, PEG has no effect on the particles growth in the absence of sonication.

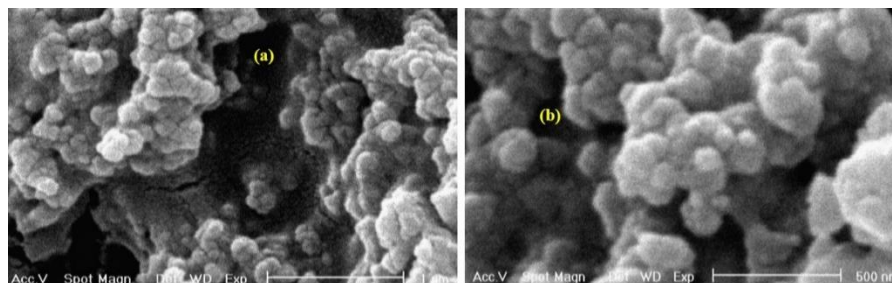


Figure 6. SEM images of $\text{Ni}(\text{OH})_2$ (a) without sonication and (b) in presence of PEG without sonication.

Fig. 7a shows the SEM images of the NiO particles for sample number 1 and Fig. 7b for sample number 7 after heating at 500°C that exhibits small and spherical NiO particles with good separation for sample No.7.

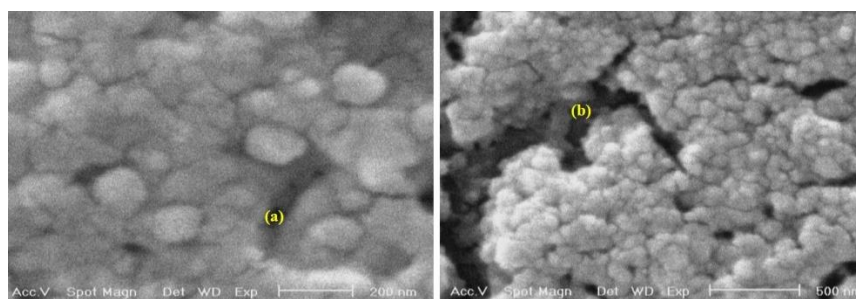


Figure 7. SEM image of NiO sample nanoparticle a) sample NO.1 b) sample NO.7.

To investigate the size distribution of the nanoparticles a particle size histogram was prepared for sample 7 after heating at 500°C, (Fig. 8). Most of the particles possess sizes in the range from 50 to 80 nm.

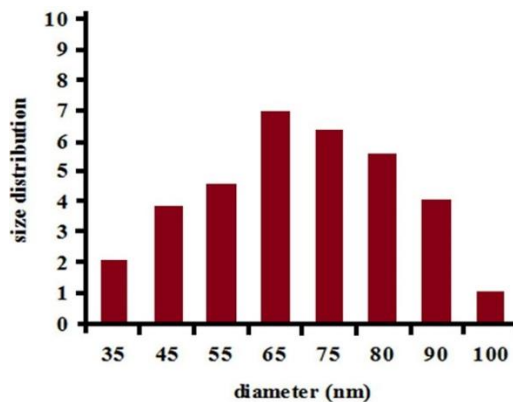


Figure 8. Particle size histogram of NiO (sample No. 7).

For further demonstration, the EDAX was performed for the sample No. 5. The EDAX spectrum given in Fig. 9 shows the presence of Ni and O as the only elementary components.

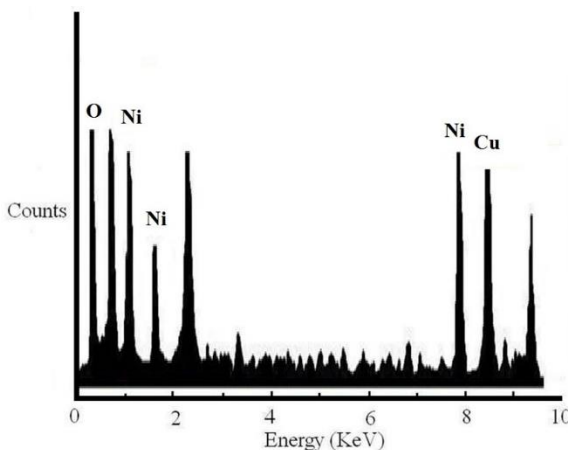


Figure 9. EDAX analysis of sample No. 5.

The sonochemical method comparing with the other methods which have been used for preparing the NiO nanostructures, is very fast and it doesn't need high temperatures during the reactions, using the surfactants is not necessary for this method and the other advantage of using ultrasound radiation is that it yields smaller particles. The effects of ultrasound radiation on chemical reactions are due to the very high temperatures and pressures that develop during the sonochemical cavity collapse by acoustic cavitation. There are two regions of sonochemical activity, the inside of the collapsing bubble, and the interface between the bubble and the liquid, which extends to about 200 nm from the bubble surface. If the reaction takes place inside the collapsing bubble, as is the case for transition metal carbonyls in organic solvents, the temperature inside the cavitation bubble can be from 5100 to 2300 K depending on the vapor pressure of the solvent. If water is used as the solvent, the maximum bubble core temperature that can be attained is close to 4000 K. The product obtained in this case will be amorphous as a result of the high cooling rates ($>1010 \text{ K.S}^{-1}$) reached during collapse. On the other hand, if the reaction takes place at the interface, where the temperature has been measured to be 1900 K, one expects to get nanocrystalline products.

If the solute is ionic, and hence has a low vapor pressure, then during sonication the amount of the ionic species will be very low inside the bubble and little product is expected to occur inside the bubbles. Since in the present study the solute is ionic, and we get nanocrystalline nickel hydroxide particles, we propose that the formation of the hydroxide particles occurs at the interface between the bubble and the liquid and the ultrasound accelerated the formation of $\text{Ni}(\text{OH})_2$.

Optical absorption spectrum of the NiO nanoparticle is represented in fig 10. The optical absorption peak intensity is found at 3.75eV (330nm). From the curve we can calculate the band gap (E_g) energy of the sample by the following equation [28].

$$(\alpha h\nu)^n = B(h\nu - E_g)$$

In which $h\nu$ is photo energy, α is absorption coefficient, B is a material constant and n is either 2 for a direct band gap material or $\frac{1}{2}$ for indirect band gap materials. Using equation (1) and taking the value $n = 2$, we can determine the corresponding band gap of the sample and the band gap energy of the NiO sample has been found to be 2.92 eV. It is interesting to notice that the value of band gap energy is lower than the energy reported by Boschloo [29] and Z Zhang [30]. Here it is also observed that NiO nanoparticle is almost transparent in visible region and shows almost sharp absorbance peak around 3.75 eV. The value $n = \frac{1}{2}$ does not produce any meaningful data for the band gap energy which corresponds that NiO is a direct band gap type semiconductor.

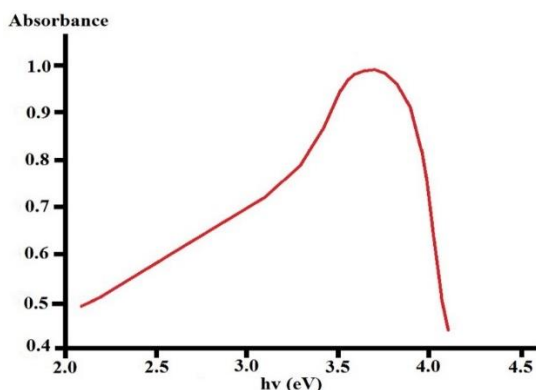


Figure.10: UV-Vis absorbance curve of NiO nanoparticles.

Fig. 11 shows the photoluminescence response curve of the sample. The PL characteristics were examined by exciting the sample with incident light of energy 4.12 eV (300 nm) and 3.99 eV (310 nm). The resulting emission characteristics show the origination of one main emission peak centered at around 3.62 eV (341 nm) with two other weak peaks at 3.77 eV (328 nm) and 3.46 eV (357 nm). The origin of the main peak associated with two feeble shoulders is attributed to the electronic transition of the Ni^{2+} ions. Optical absorption study reveals the existence of several transitions at energies below band gap in NiO [31]. Adler and Feinleib [32] reported a series of absorption peaks below 4 eV as purely interionic 3d8-3d8 transitions of Ni^{2+} . The study of electron energy loss spectroscopy (EELS) and spin polarized electron energy loss spectroscopy (SPEELS) also confirm the existence of this kind of transition of the 3d8 electrons in NiO [33, 34]. Here also the luminescence peak of NiO sample is coming from the electronic transition of the cationic state and one can exploit this property of NiO nanoparticle as a good emitter of 341 nm (3.62 eV) wavelengths.

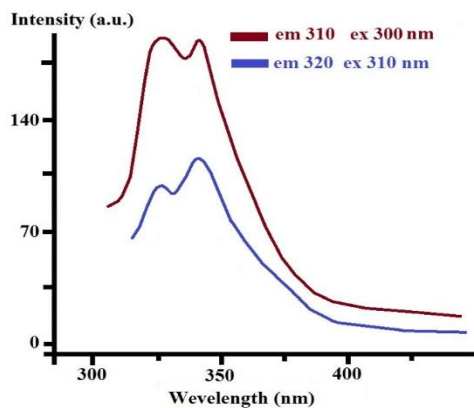


Figure.11: PL-spectra NiO nanoparticles at excitation wavelength 300 nm and 310 nm.

4 Conclusions

We have successfully synthesized nano crystalline Ni(OH)₂ and NiO through a sonochemical reaction between different concentration of Ni(CH₃COO)₂·2H₂O and NaOH with different aging times and different sonicated powers. In similar study CdCO₃ nanoparticles were obtained from reaction of Cd(CH₃COO)₂ with TMAH under ultrasonic condition. The reactions proceeded under ultrasonic conditions resulting in spherical and uniform NiO and Ni(OH)₂ nano crystallites as shown by SEM observation. Comparing with the wet chemical routes such as hydrothermal or solvothermal methods this sonochemical method does not require pressure controlling and high temperature. Comparing with template-assisted method that requires surfactant and pH value controlling, this procedure does not need any surfactant and control of pH values. There are several reports about the synthesis of NiO nanostructures so far. Different methods may still be considered for the preparation of NiO films, such as dehydration of laser-ablated Ni(OH)₂ layers. Nickel oxide films have also been obtained by atomic layer deposition (ALD) process from nickel h-diketonate, CO₂ and ozone. The recrystallization of NiO from Ni(OH)₂ was observed at 500°C in air. By heating Ni(OH)₂ at 500°C the NiO nanopowders were obtained and the XRD phase analysis showed the formation of NiO with the Cubic symmetry. This method can be easily controlled and is expected to be applicable to the fabrication of other nano sized particles.

Acknowledgements

Supporting of this investigation by Lorestan University, Khorramabad, IRAN is gratefully acknowledged.

References

- [1] S.R. Ovshinsky, M.A. Fetcenko, J. Ross, *Science* 260 (1993) 176.
- [2] A. Taniguchi, N. Fujikoka, M. Ikoma, A. Ohta, *J. Power Sources*, 100 (2001) 117.
- [3] K. Bande, T. Gamnke, *Adv. Mater.* 2 (1990) 10.
- [4] R.S. Jayashree, P.V. Kamath, *J. Appl. Electrochem.* 29 (1999) 449.
- [5] D.L. Chen, L. Gao, *Chem. Phys. Lett.* 405 (2005) 159.
- [6] P. Jeevanandam, Y. Koltypin, A. Gedanken, *Nano. Lett.* 1 (2001) 263.
- [7] D.N. Yang, R.M. Wang, M.S. He, J. Zhang, Z.F. Liu, *J. Phys. Chem. B*, 109 (2005) 7654.
- [8] M. Keitaro, K. Takashi, T. Akira, *Adv. Mater.* 14 (2002) 1216.
- [9] X.J. Han, P. Xu, C.Q. Xu, L. Zhao, Z.B. Mo, T. Liu, *Electrochim. Acta*, 50 (2005) 2763.
- [10] X.H. Liu, L. Yu, *J. Power Sources* 128 (2004) 326.
- [11] Z.H. Liang, Y.J. Zhu, X.L. Hu, *J. Phys. Chem. B* 108 (2004) 348.
- [12] D.B. Wang, C.X. Song, Z.S. Hu, X. Fu, *J. Phys. Chem. B* 109 (2005) 1125.
- [13] J. He, H. Lindström, A. Hagfeldt, S.E. Lindquist, *J. Phys. Chem. B*, 103 (1999) 8940.
- [14] B. Pejova, T. Kocareva, M. Najdoski, I. Grozdanov, *Appl. Surf. Sci.* 165 (2000) 271.
- [15] Y.W. Tan, S. Srinivasan, K.S. Choi, *J. Am. Chem. Soc.* 127 (2005) 3596.
- [16] M.H. Cao, X. He, J. Chen, C.W. Hu, *Cryst. Growth Des.* 7 (2007) 170.
- [17] B.H. Liu, S.H. Yu, S.F. Chen, C.Y. Wu, *J. Phys. Chem. B* 110 (2006) 4039.
- [18] E.L. Miller, R.E. Rocheleau, *J. Electrochem. Soc.* 144 (1997) 3072.
- [19] K. Bange, T. Gamnke, *Adv. Mater.* 2 (1990) 10.
- [20] X. Zhang, G. Chen, *Thin Solid Films* 298 (1997) 53.
- [21] B. Sheela, H. Gomathi, G.P. Rao, *J. Electroanal. Chem.* 394 (1995) 267.
- [22] R.C. Makkus, K. Hemmes, J.H.W.D. Wir, *J. Electrochem. Soc.* 141 (1994) 3429.
- [23] S. Deki, Y. Aoi, *J. Mater. Res.* 13 (1998) 883.
- [24] T.J. Richardson, M.D. Rubin, *Electrochim. Acta* 46 (2001) 2119.
- [25] H. Nagayama, H. Honda, H. Kawahara, *J. Electrochem. Soc.* 135 (1988) 2013.

- [26] S. Deki, Y. Aoi, J. Okibe, H. Yanagimoto, A. Kajinami, *J. Mater. Chem.* 7 (1997) 1769.
- [27] B. Pejova, T. Kocareva, M. Najdoski, I. Grozdanov, *Appl. Surf. Sci.* 165 (2000) 271.
- [28]. J. I. Pancove 1971 *Optical Processes in Semiconductors* (Englewood Cliffs, NJ: Prentice Hall)
- [29]. G. Boschloo and A. Hagfeldt 2001, *J Phys. Chem. B*, 105, 3039
- [30]. X. Wang, J. Song, L. Gao, J. Jin, H. Zheng and Z. Zhang 2005 *Nanotechnology* 16 37-39
- [31]. T. Tsuboi and W. Kleeman 1994 *J. Phys.: Condensed Matter* 6 8625
- [32]. D. Adler and J. Feinleib 1970 *Phys. Rev. B*, 2, 3112 A.
- [33]. Gorschluter and H. Merz 1994 *Phys. Rev. B*, 49, 17293,
- [34]. B. Fromme, M. Moller, Th. Anschutz, C. Bethke and E. Kisker 1996 *Phys. Rev. Lett.* 77 1548.
-